

Stem Cell Reports, Volume 7

Supplemental Information

iPSC-MSCs with High Intrinsic MIRO1 and Sensitivity to TNF- α Yield Efficacious Mitochondrial Transfer to Rescue Anthracycline-Induced Cardiomyopathy

Yuelin Zhang, Zhendong Yu, Dan Jiang, Xiaoting Liang, Songyan Liao, Zhao Zhang, Wensheng Yue, Xiang Li, Sin-Ming Chiu, Yuet-Hung Chai, Yingmin Liang, Yenyen Chow, Shuo Han, Aimin Xu, Hung-Fat Tse, and Qizhou Lian

Figure S1. Linked to Figure 1

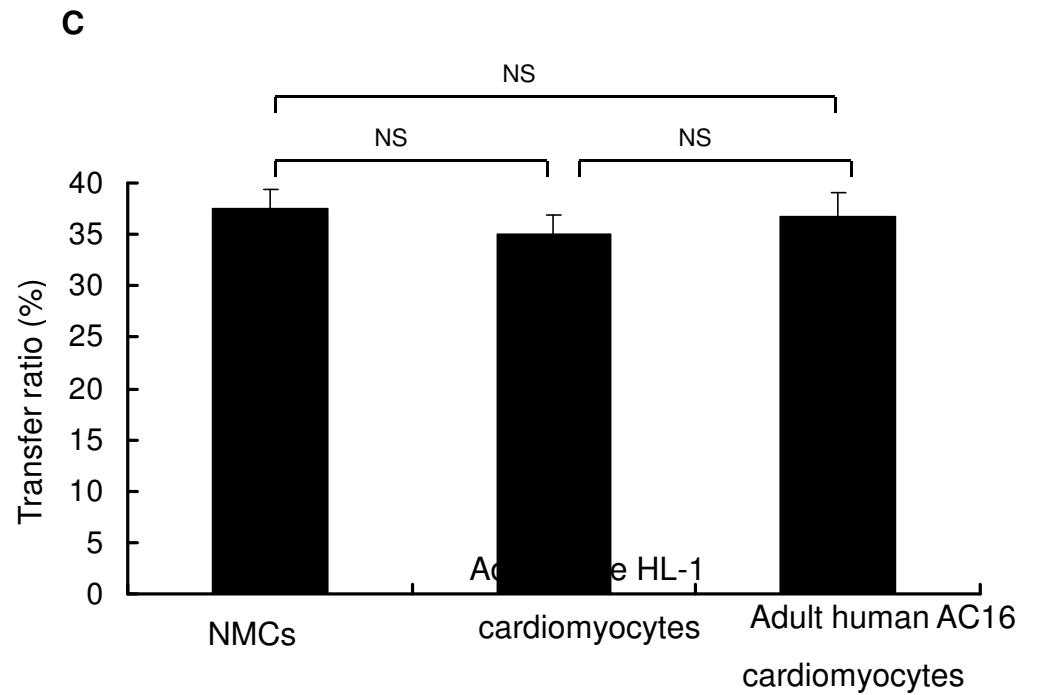
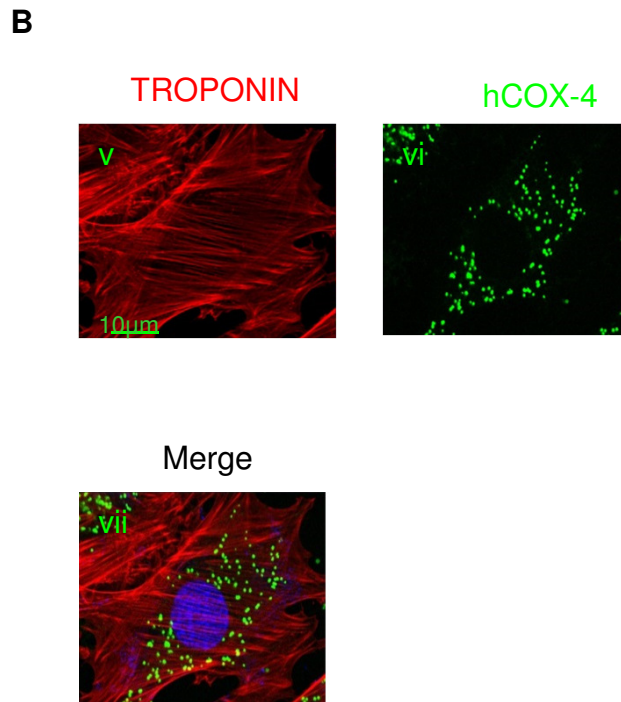
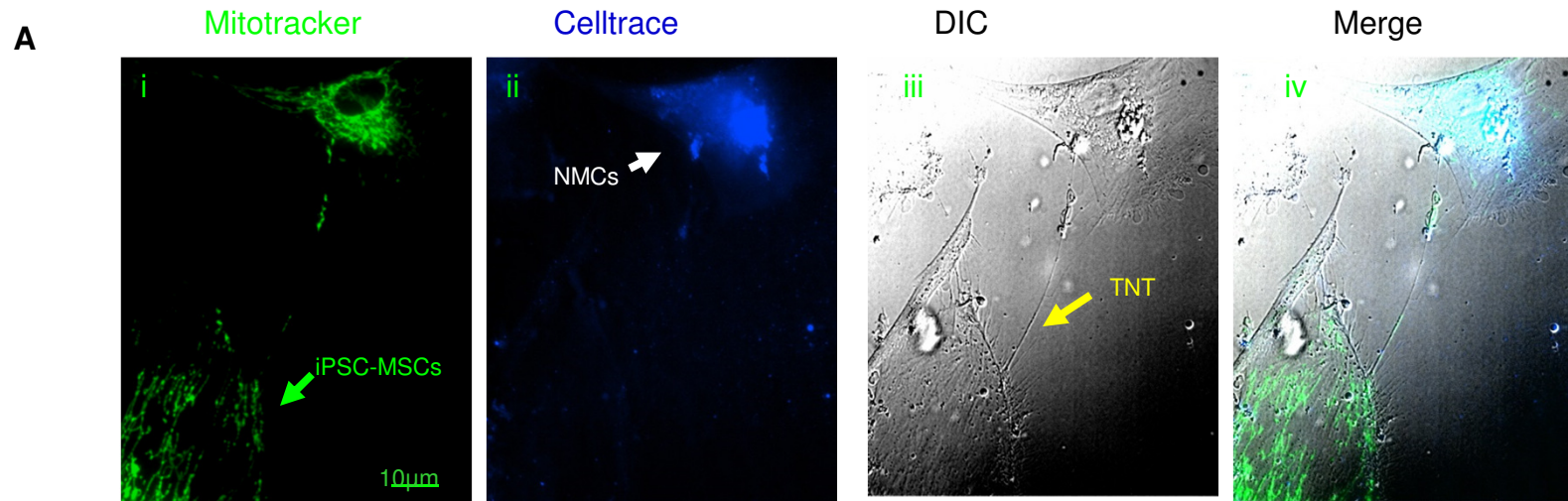


Figure S2. Linked to Figure 2

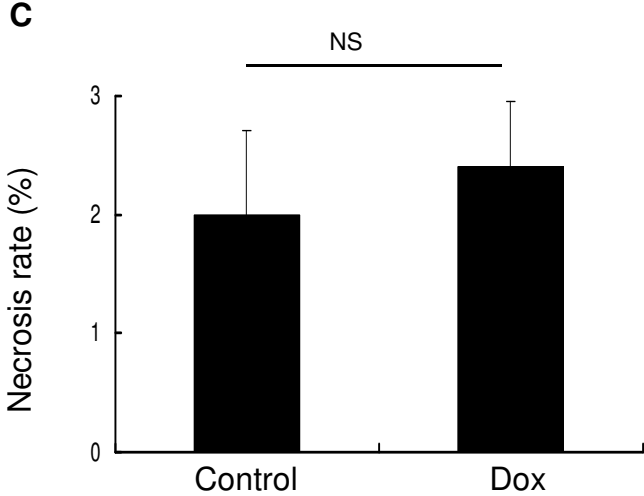
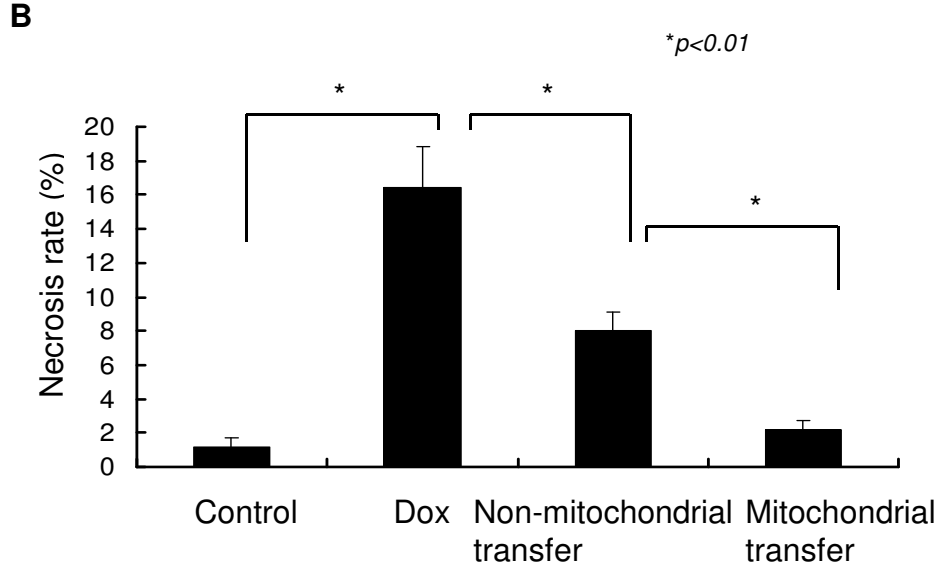
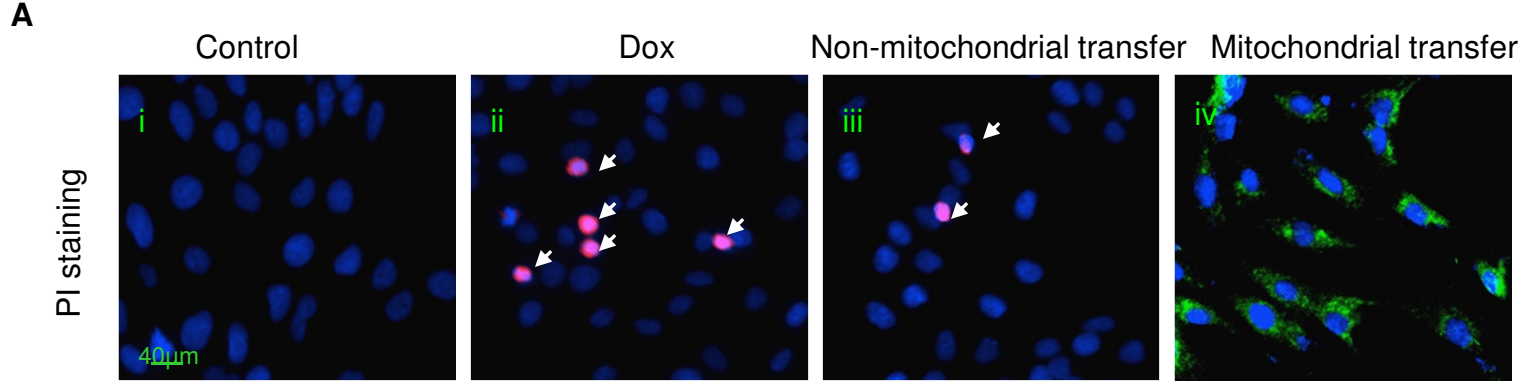


Figure S3. Linked to Figure 3

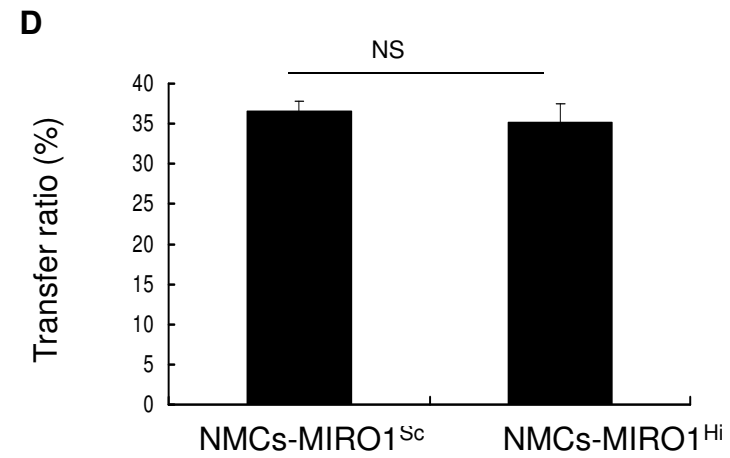
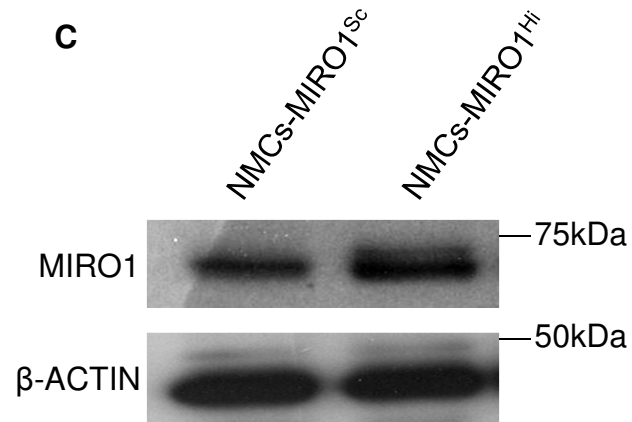
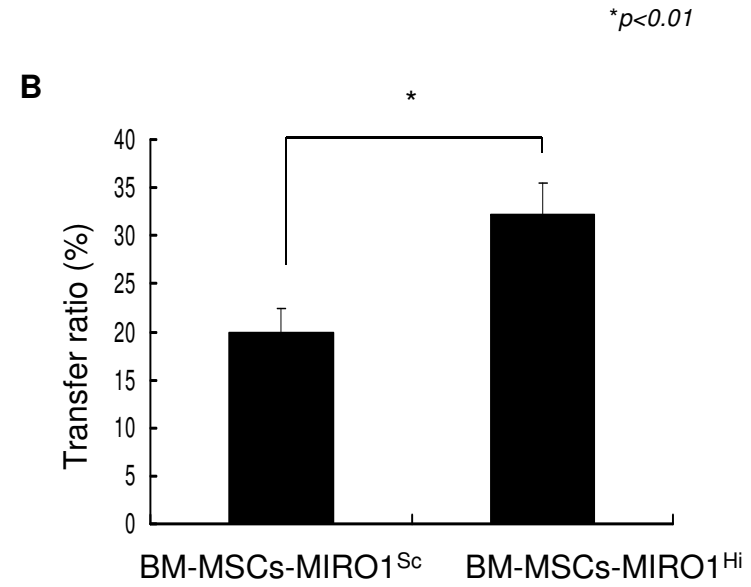
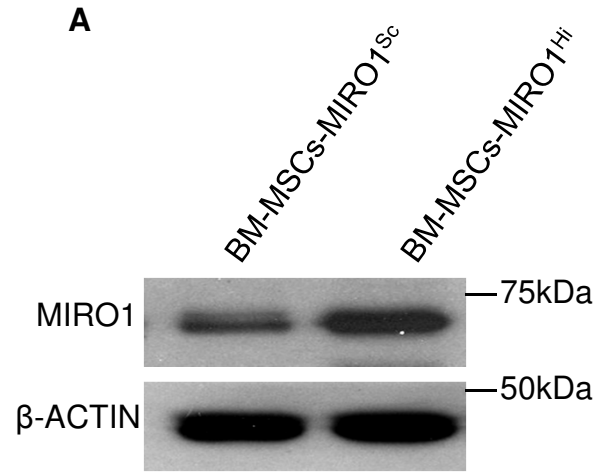


Figure S4. Linked to Figure 4

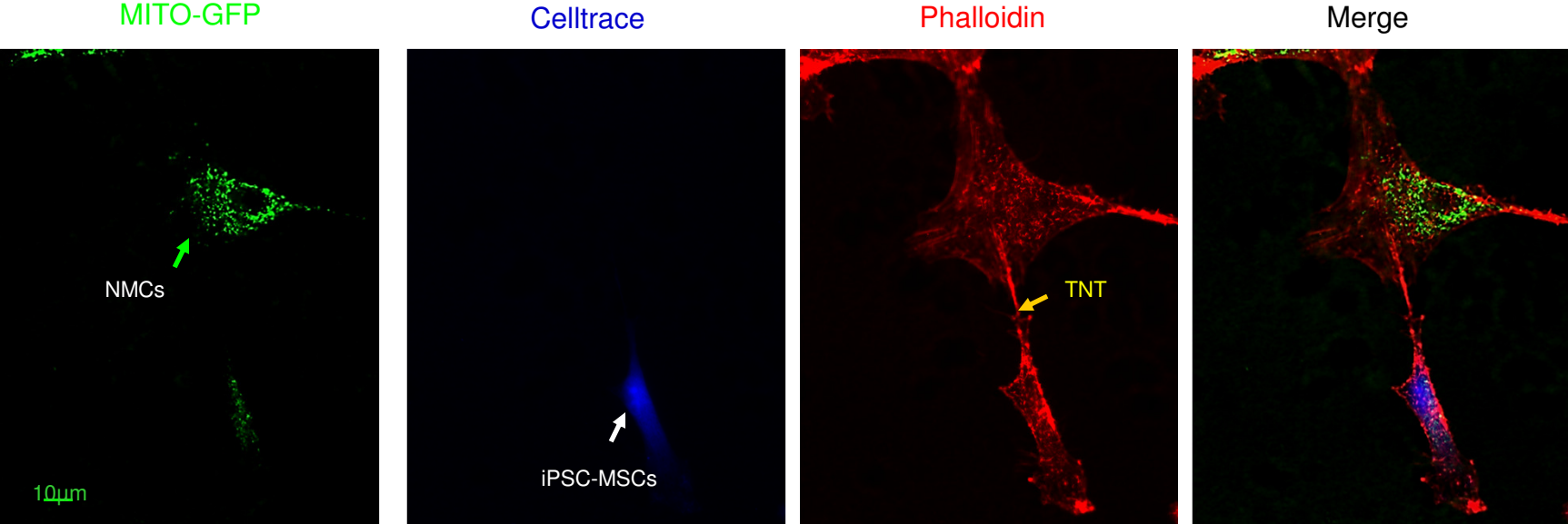


Figure S5. Linked to Figure 5

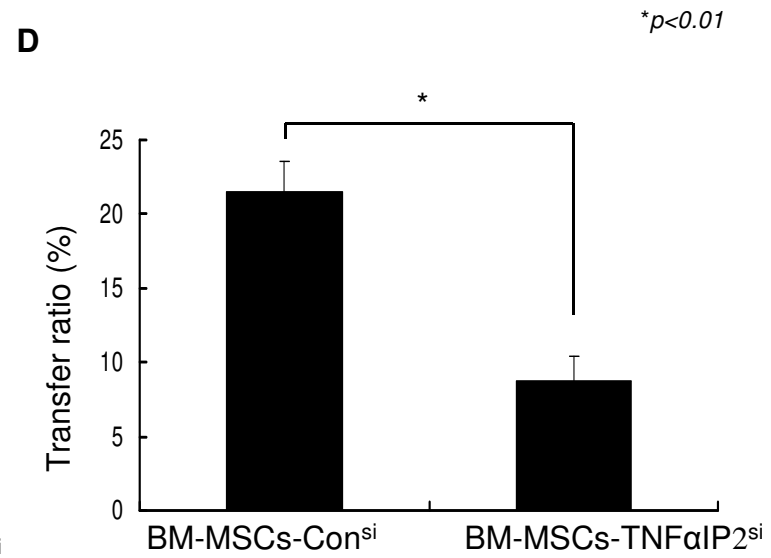
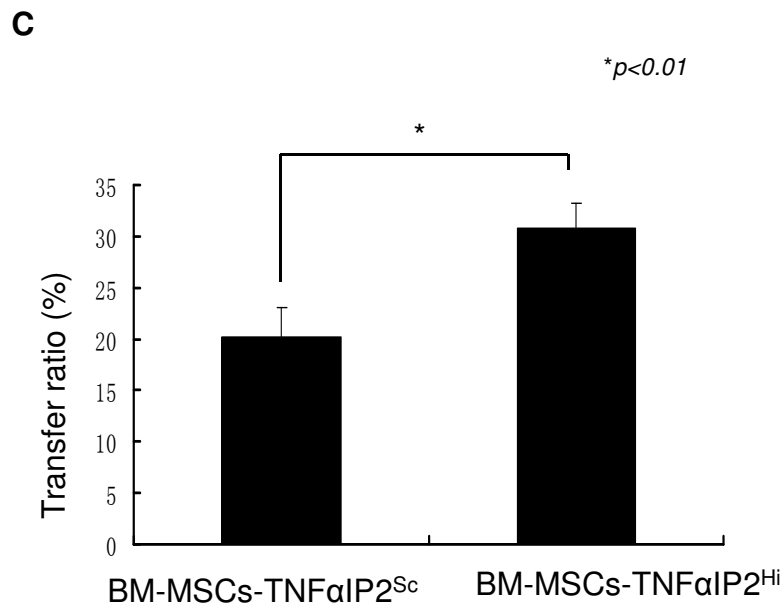
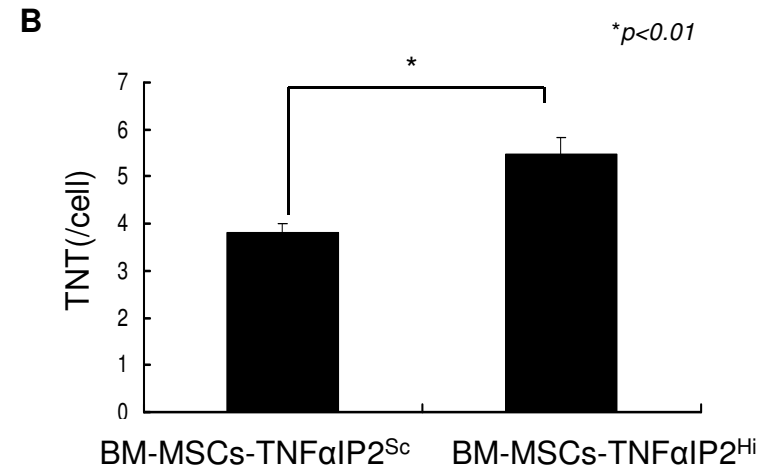
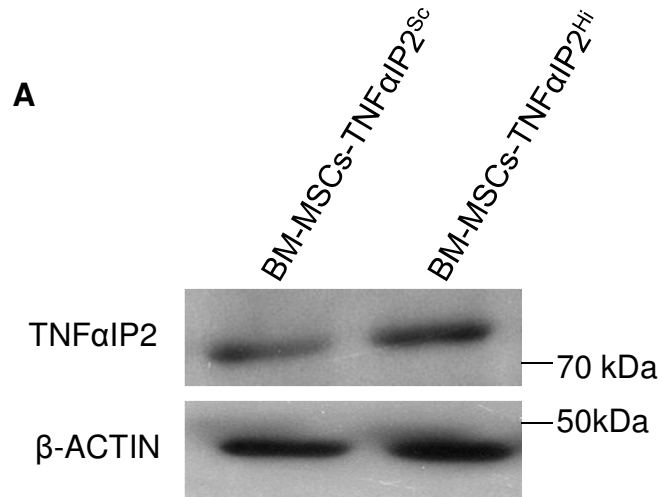
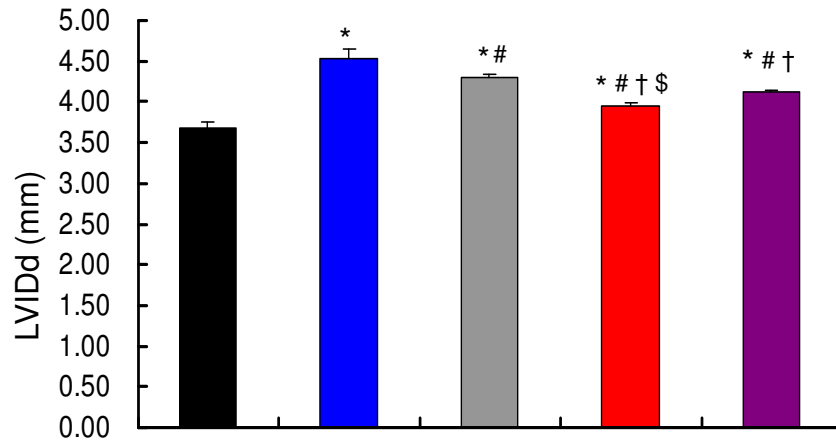


Figure S6. Linked to Figure 6

■ Control
■ Dox
■ BM-MSCs
■ iPSC-MSCs
■ iPSC-MSCs-TNF α IP2^{si}

* $p < 0.01$ vs Control
$p < 0.01$ vs Dox
† $p < 0.01$ vs BM-MSCs
§ $p < 0.01$ vs iPSC-MSCs-TNF α IP2^{si}

A



B

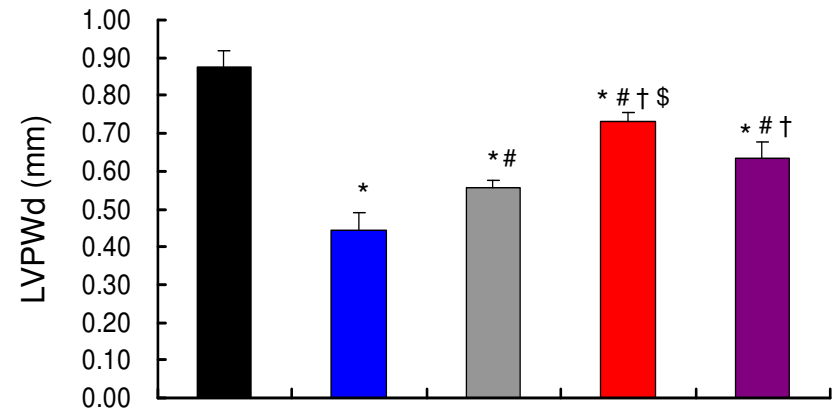
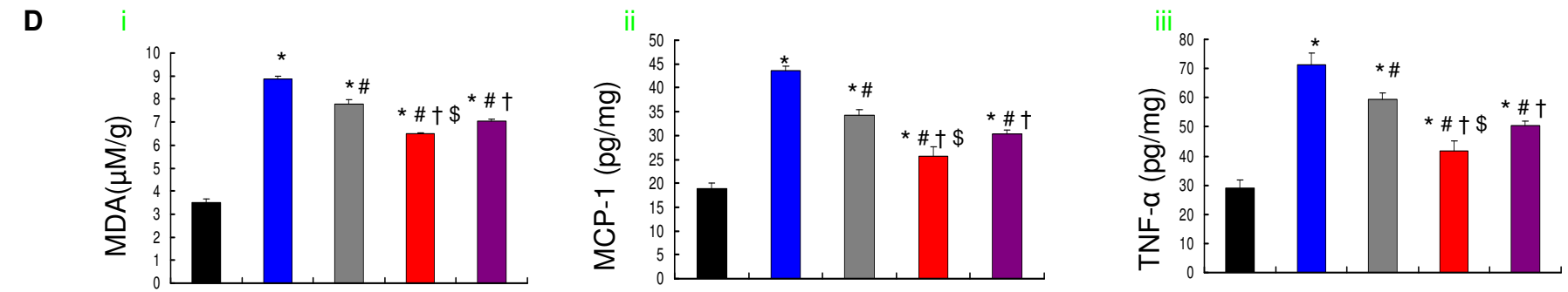
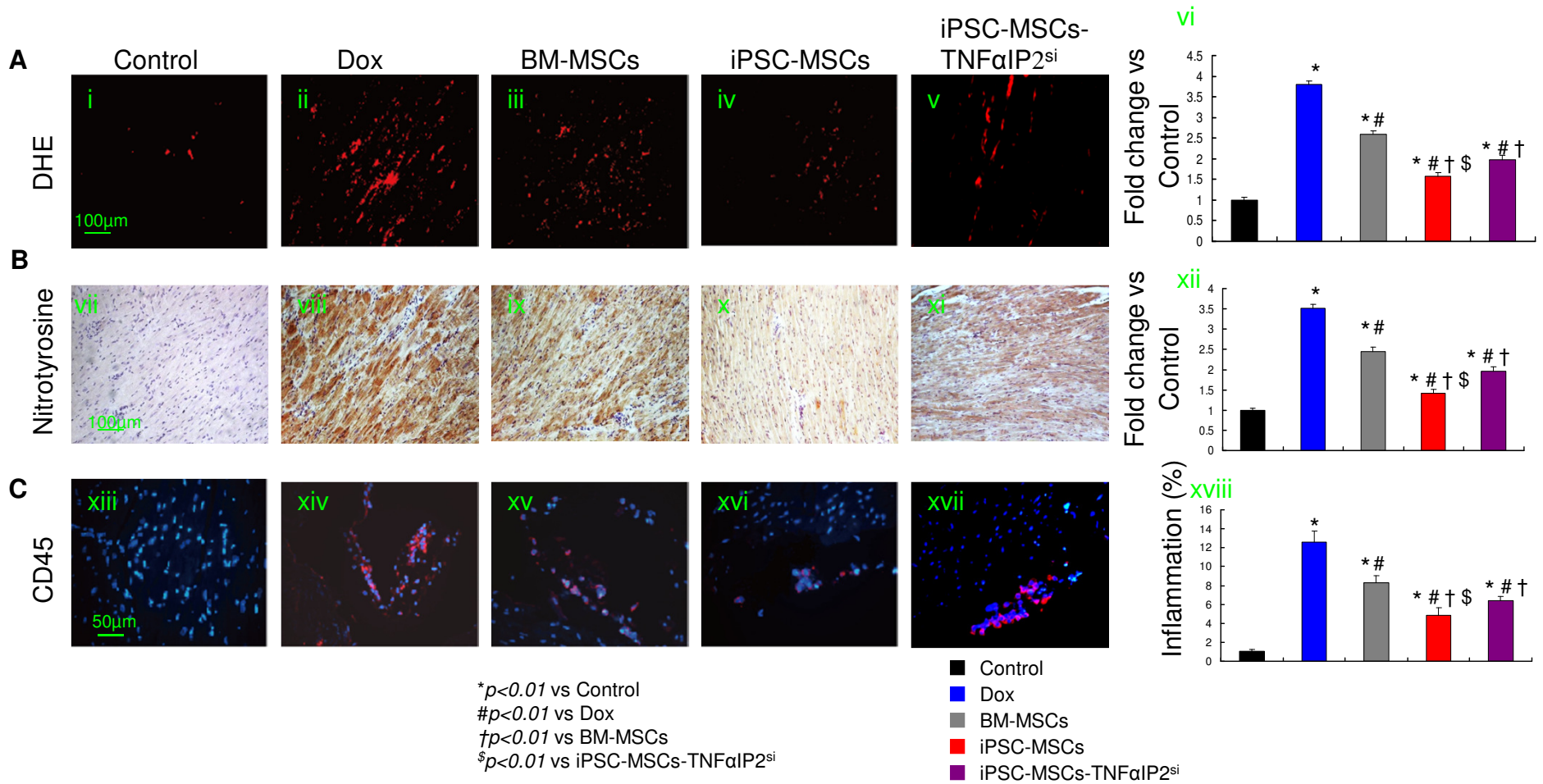


Figure S7. Linked to Figure 7



Supplemental figure legends:

Figure S1. Linked to Figure 1

Mitochondrial transfer from iPSC-MSCs to NMCs A) Representative images of mitochondrial transfer from iPSC-MSCs to NMCs. i) Mitotracker labeling. ii) Celltrace labeling. iii) DIC iv) Merge. B) Co-culturing NMCs with iPSC-MSCs for 24h, immunostaining with anti-TROPONIN and anti-human COX-4 in NMCs showed that NMCs contained human mitochondria (v-vii). C) Mitochondrial transfer ratio between iPSC-MSCs and stressed NMCs, adult mice HL-1 cardiomyocytes or human adult AC16 cardiomyocytes.

Data represent the means \pm SD of three independent experiments. NS, not significant.

Figure S2. Linked to Figure 2

Mitochondrial transfer from iPSC-MSCs to NMCs reduces Dox-induced NMC necrosis A) Representative images of PI staining showing the necrosis of NMCs among control (i), doxorubicin (Dox, ii), Non-mitochondrial transferred-NMCs (iii), mitochondrial transferred-NMCs (iv) groups. Arrows show the necrotic NMCs. B) The necrotic rate of NMCs among the different groups was analyzed. C) Dox did not induce necrosis of MSCs after 24 hours challenge.

Data represent the means \pm SD of three independent experiments. * $p < 0.01$. NS, not significant.

Figure S3. Linked to Figure 3

Overexpression of MIRO1 by BM-MSCs contributes to mitochondrial transfer from

MSCs to NMCs under Dox challenge A) MIRO1 was measured in BM-MSCs transfected with control plasmid (BM-MSCs-MIRO1^{Sc}) and MIRO1 cDNA plasmid (BM-MSCs-MIRO1^{Hi}). B) Mitochondrial transfer ratio between BM-MSCs-MIRO1^{Sc} or BM-MSCs-MIRO1^{Hi} and stressed NMCs was measured by FASC.

Data represent the means \pm SD of three independent experiments. * $p < 0.01$.

Overexpression of MIRO1 in NMCs has no impact on mitochondrial transfer from MSCs to NMCs C) MIRO1 was measured in NMCs transfected with control plasmid (NMCs-MIRO1^{Sc}) and MIRO1 cDNA plasmid (NMCs-MIRO1^{Hi}). D) Mitochondrial transfer ratio between iPSC-MSCs and stressed NMCs-MIRO1^{Sc} or NMCs-MIRO1^{Hi} was measured by FASC.

Data represent the means \pm SD of three independent experiments. NS, not significant.

Figure S4. Linked to Figure 4

Mitochondrial transfer from NMCs to iPSC-MSCs is mediated by tunneling nanotubes The MITO-GFP labeled NMCs were co-cultured with celltrace labeled iPSC-MSCs under Dox. Twenty four hours later, phalloidin staining was performed. Representative images of TNT formation and mitochondrial transfer between NMCs and iPSC-MSCs. i) MITO-GFP labeling. ii) Celltrace labeling. iii) Phalloidin staining showing TNT formation between NMCs and iPSC-MSCs. iv) Representative images illustrating mitochondrial transfer from NMCs to iPSC-MSCs via TNT.

Figure S5. Linked to Figure 5

Overexpression of TNF α IP2 in BM-MSCs contributes to mitochondrial transfer from

MSCs to NMCs. A) TNF α IP2 was measured in BM-MSCs transfected with control plasmid (BM-MSCs-TNF α IP2^{Sc}) and TNF α IP2 cDNA plasmid (BM-MSCs- TNF α IP2^{Hi}). B) The TNT formation by BM-MSCs-TNF α IP2^{Sc} and BM-MSCs- TNF α IP2^{Hi} under TNF- α stimulation was calculated. C) Mitochondrial transfer ratio between BM-MSCs-TNF α IP2^{Sc} or BM-MSCs-TNF α IP2^{Hi} and stressed NMCs was measured by FASC. D) Mitochondrial transfer ratio between BM-MSCs-Con^{Si} or BM-MSCs-TNF α IP2^{Si} and stressed NMCs was measured by FASC.

Data represent the means \pm SD of three independent experiments. *p<0.01.

Figure S6. Linked to Figure 6

iPSC-MSCs transplantation alters the morphology of heart induced by Dox. A) Left ventricular internal diameter end diastole (LVIDd) among the different groups was analyzed group (n=6 mice per group).

B) Left ventricular posterior wall end diastole (LVPWd) among the different groups was analyzed group (n=6 mice per group).

Data represent the means \pm SD. * p<0.01 vs. Control; #p<0.01 vs. Dox; † p<0.01 vs. BM-MSCs; §p<0.01 vs. iPSC-MSCs-TNF α IP2^{Si}.

Figure S7. Linked to Figure 7

Transplantation of iPSC-MSCs ameliorates Dox-induced oxidative stress and inflammation *in-vivo*. A) Representative images showing fluorescent intensity of dihydroethidium (DHE) among control (i), doxorubicin (Dox, ii), BM-MSCs (BM-MSCs, iii), iPSC-MSCs (iPSC-MSCs, iv) or iPSC-MSCs-TNF α IP2^{Si} (iPSC-MSCs-TNF α IP2^{Si}, v)

treatment groups. Quantitative measurement of DHE fluorescent intensity among experimental groups after being normalized to the control group (vi). B) Representative images showing different levels of 3-nitrotyrosine immunoactivity among control (vii), doxorubicin (Dox, viii), BM-MSCs treatment (BM-MSCs, ix), or iPSC-MSCs (iPSC-MSCs, x) or iPSC-MSCs-TNF α IP2^{si} (iPSC-MSCs-TNF α IP2^{si}, xi) treatment groups. Quantitative measurement of 3-nitrotyrosine immunofluorescent intensity among different experimental groups after being normalized to control group (xii). C) Representative images showing differential accumulation of inflammatory cells by immunofluorescence for leukocyte common antigen CD45 among control (xiii), doxorubicin group (Dox, xiv), BM-MSCs group (BM-MSCs, xv), iPSC-MSCs group (iPSC-MSCs, xvi) and iPSC-MSCs-TNF α IP2^{si} group (iPSC-MSCs-TNF α IP2^{si}, xvii). Quantitative measurement of inflammation among different experimental groups (xviii). Quantitative measurement of DHE (A-vi) or 3-nitrotyrosine level (B-xii) is expressed as fold-change and normalized to control group. Quantitative measurement of CD45 (C-xviii) is expressed as percent of positive staining versus total per myocardium area group (n=6 mice per group).

D) At 3-weeks after cell transplantation, ROS generation and inflammatory cytokine in heart tissue from different experimental groups were measured. i) MDA concentration, ii) MCP-1 concentration, iii) TNF- α concentration group (n=6 mice per group).

Data represent the means \pm SD. * p<0.01 vs. Control; #p<0.01 vs. Dox; †p<0.01 vs. BM-MSCs; §p<0.01 vs. iPSC-MSCs-TNF α IP2^{si}.

Supplemental Videos: Time lapse videos showing mitochondria movement is through these TNTs connecting iPSC-MSCs and NMCs.

Video S1: Camera phase of time-lapse video showed mitochondria were being transferred from MSCs to NMCs.

Video S2: MITO-GFP labeled MSCs were co-cultured with celltrace labeled NMCs under Dox challenge. Time-lapse video shows the GFP-mitochondria were moving from MSCs to NMCs. Red arrow shows the moving mitochondria.

Table S1: Tumor Formation of iPSC-MSCs in SCID Mice

Cell Type	IMR90-iPSC-MSCs		Lee NL-iPSC-MSCs		BM-MSCs		Hep3B
Passages	P6	P30	P16	P27	P4	P7	P52
Cell No.	1×10^5	1×10^5	1×10^5	1×10^5	1×10^5	1×10^5	1×10^5
SC Injections	8	8	8	8	8	8	8
IM Injections	8	8	8	8	8	8	8
IT injections	8	8	0	0	0	0	0
Months	4	4	4	4	4	4	4
Tumor Formation	0	0	0	0	0	0	16

The risk of tumor formation was assessed by injection of iPSC-MSCs, BM-MSCs and Hep3B tumor cell line into Severe Combined Immunodeficiency Mice (SCID mice, n=8, each group). Each mouse received 1×10^5 cells at each site of subcutaneous (SC), intramuscular (IM) and intratesticular (IT) injection. After 4 months of cell injections, mice were sacrificed and the injected sites were examined to check tumor formation.

Supplemental Experimental Procedures

Cell culture

BM-MSCs and iPSC-MSCs were cultured with DMEM plus 10% fetal bovine serum (GIBCO), basic fibroblast growth factor (bFGF, 5ng/mL), and epidermal growth factor (EGF, 10ng/mL). Primary NMCs were obtained and cultured as previously reported (Chan et al., 2010). HL-1 cells, generously provided by Dr. William Claycomb (Louisiana State University Health Science Center, New Orleans, LA, USA) (Claycomb et al., 1998), were maintained in modified Claycomb medium (Sigma-Aldrich) supplemented with 10% fetal bovine serum (GIBCO), 100 µg/ml penicillin-streptomycin, 0.1 mM norepinephrine, and 2 mM L-glutamine. Adult human ventricular cardiomyocyte AC16 cells were cultured in DMEM F-12 supplemented with 12.5% fetal bovine serum (GIBCO)(Davidson et al., 2005). Cells were diluted at a ratio of 1:4 when they reached confluence. Moreover, in-vitro co-culture experiments of NMCs, adult mice and human cardiomyocytes with MSCs were performed with and without Dox treatment. 5×10^5 NMCs were labeled with 1µM celltrace violet (Molecular Probes) for half an hour and washed with fresh medium. After washing and resting, MITO-GFP-MSCs and labeled NMCs were re-suspended in mixed medium and co-cultured at a 1:1 ratio in 24-well plates with cover slips in the presence of 1µM Dox. After 24 hours, the cells were washed with PBS and stained by phalloidin-rhodamine (5mg/mL, Sigma-Aldrich) and then visualized by laser confocal scanning microscopy (Zeiss LSM Meta 510).

Histological analysis

After echocardiographic and hemodynamic studies, mice were sacrificed. The hearts were harvested and fixed with 10% buffered formalin and then embedded in paraffin, and finally sectioned to 5- μ m slides. Hematoxylin and eosin staining and Sirius red staining were performed. The degree of fibrosis was expressed as a percentage of the whole heart, and was measured by two independent investigators. The size of the fibrotic area was quantified with 6 randomly chosen high-power fields for each heart section, 6 mice for one group.

Animal model

Echocardiography was performed one week following the last Dox injection to confirm successful creation of an AIC model. Briefly, mice were anesthetized (intra-peritoneal injection of 100mg/kg of ketamine and 20mg/kg of xylazine) and echocardiographic parameters were measured with a high resolution Micro-Ultrasound system (Vevo 770, Visual Sonics Inc.) equipped with a 25-MHz linear transducer. Left ventricular (LV) diameter and diastolic and systolic posterior wall thickness were measured and then the ejection fraction (EF) was calculated.

Three weeks after cell transplantation, and after echocardiographic measurement, hemodynamic measurements were performed. Briefly, a 1.4-Fr high-fidelity microtip catheter connected to a pressure transducer (Millar Instruments, Houston, TX, USA) was inserted into the LV cavity via the internal jugular artery to evaluate LV pressure and $\pm dp/dt$ using the Power Lab system (AD Instruments, Inc., Colorado Springs, CO,

USA). All mice were then sacrificed, and histological examination to assess myocardial fibrosis, immunohistochemical staining, apoptosis and oxidative stress were performed.

Immunohistochemical staining

Immunohistochemical staining was performed according to the protocol. Briefly, following incubation with 5% bovine serum albumin for 30mins, heart sections were stained with primary antibodies and incubated overnight at 4°C with a 1:100 dilution. The antibodies used in this study included anti-GFP (SC-8334, Santa Cruz), anti-human nuclear antigen (HNA) (MAB1281, Chemicon), anti-CD45 (553081, BD PharMingen), anti-TROPONIN (MA5-12960, ThermoFisher Scientific), anti-COX-4 (SC-133478, Santa Cruz), anti-NITROSYNE3 (Rockland, 200-301-A98). Negative control reactions were incubated with phosphate-buffered saline instead of the primary antibody. The second antibody with FITC-conjugated anti-mouse IgG (1:1000), anti-rabbit IgG (1:1000) or anti-goat IgG (1:1000) was then used against the primary antibodies and incubated for 1 hr at room temperature. Finally, heart sections were washed and mounted with 4, 6-diamidino-2-phenylindole (DAPI) to stain the nucleus. Six mice from each group were analyzed; five sections were randomly collected from each mouse and then analyzed with a deconvoluted fluorescent microscope and Image J software.

TUNEL assay

According to the manufacturer's instructions, terminal deoxynucleotidyl transferase mediated dUTP nick end-labeling (TUNEL) staining was carried out to detect apoptotic cells in the heart. Briefly, heart sections were washed and incubated with 1µg/mL Proteinase K/10mM Tris solution for 15mins at room temperature and washed twice in PBS and finally incubated with 100µL TUNEL reaction mixture in a humidified chamber for 1hr at room temperature. Sections were then washed 3 times with PBS, mounted with DAPI, observed under a fluorescent microscope and finally photographed. Six mice from each group were analyzed; five sections were randomly collected from each mouse and viewed for positive tunnel cell numbers.

DHE staining

The presence of superoxide anion (O₂⁻) oxygen radicals generated by doxorubicin in the heart was evaluated by Dihydro-ethidium (DHE) staining. Briefly, the heart sections were incubated with DHE (2x10⁻⁶ mol/L) at room temperature for 30mins. DHE fluorescence was captured by a fluorescent microscope with 585nm filter. Fluorescence intensity was expressed as arbitrary fluorescence units (AFU) and measured with Image J software. Six mice from each group and five sections from each mouse were analyzed.

Determination of oxidative stress and inflammatory markers

Following the manufacturer's instructions, the concentration of MDA in the heart tissue from different experimental groups was measured by Thiobarbituric Acid

Reactive Substance Assay Kit (Cayman Chemical).

The concentrations of Monocyte chemotactic protein-1 (MCP-1) and TNF- α served as inflammatory markers in the different experimental groups and were measured using the mouse MCP-1 Elisa kit (KMC1011, Invitrogen) and mouse TNF- α Elisa kit (KMC3011, Invitrogen), respectively.

RT-PCR

RT-PCR was performed as previously described (Liang et al., 2015). Total RNA was extracted using RNeasy kit (Qiagen, 74104). 1 μ g of total RNA was used for the generation of first-strand cDNA using First-Strand cDNA Synthesis Kit (Takara, 6110) according to the protocol. Primers used in this study were as follows: *human specific mtDNA*: F:5'-CCTTCTTACGAGCCAAAA-3', R:5'-CTGGTTGACCATTGTTTG-3'; *murine specific mtDNA*: F:5'-ACTCTTCACACAAACATAA-3', R:5'-CTGGGTGATCTTTGTTTG-3'; *human ALU-SX*: F:5'-GGCGCGGTGGCTCACG-3', R:5'-TTTTTTGAGACGGAGTCTCGCTC-3'; *mice C-mos*: F: 5'- GAATTCAGATTTGTGCATACACAGTGACT -3 ' , R: 5 ' -AACATTTTTCGGGGAATAAAAAGTTGAGT-3 ' ; *TNF α IP2* : F: 5 ' -AGCATCACGCTGGACTTGGG-3 ' , R: 5 ' -CGGAAGGACAGGCAGTTGTT-3 ' . *GAPDH* was loaded as controls. PCR conditions were 36 cycles of 94° C for 1 minute, 55° C for 30 seconds, 72° C for 1 minute. The amplified products were determined by electrophoresis in 2.0% agarose gel containing ethidium bromide.

Western blot

Western blot was performed as previously described (Cheng et al., 2009). Total protein was extracted and the concentration was measured by bicinchoninic (BCA) protein assay kit and then run on 10% polyacrylamide gel. Before protein transfer, PVDF membranes were incubated with the primary antibodies overnight at 4°C and then incubated with horseradish peroxidase-conjugated anti-rabbit or anti-mouse secondary antibody at 37°C for one hr. Primary antibodies were: TNF α IP2 (SC-28318, Santa Cruz), P65NF- κ B (SC-109, Santa Cruz), P-P65 NF- κ B (SC-33020, Santa Cruz), anti-GFP (sc-9996, Santa Cruz), anti-COX-4 (SC-133478, Santa Cruz), MIRO-1 (SC-102083, Santa Cruz) and β -ACTIN (SC-47778, Santa Cruz).

siRNA intervention and plasmid transfection

TNF α IP2siRNA, control siRNA or MIRO1-shRNA (Sigma Aldrich, USA) were used with a standardized MOI (multiplicity of infection) of 5 according to the protocol. BM-MSCs were transfected with human *MIRO1* (Cat No. HG15898-CM, Sino Biological Inc) or human *TNF α IP2* (Cat No. HG15695-CM, Sino Biological Inc) plasmid according to the protocol.

In-vivo measurement of adenosine triphosphate (ATP) content

For ATP extraction, about 20 mg of frozen heart tissue was homogenized in 200 μ l ice-cold trichloroacetic acid (2.5% vol/vol in H₂O) and centrifuged at 1000 g for 10 mins at 4°C. The supernatant was neutralized with 24 μ l 1 M Tris base and used for ATP assays with the ATP Determination Kit (Molecular Probes, Invitrogen). The pellet

was neutralized in 100 μ l 0.5 M NaOH and protein concentration was measured by Bradford assay (Bio-Rad). Briefly, a reaction solution comprised of H₂O, dithiothreitol, D-luciferein and firefly luciferase was prepared. 10 μ l of sample or ATP standard was added to 100 μ l reaction solution and luminescence intensity around 560 nm was determined. The ATP amount was adjusted by the protein concentration for final result.

Assessments of mitochondrial transfer

Mitochondrial targeting transfection

Mitochondrial targeting green fluorescence protein (pCT-MITO-GFP, Cat: Cyto102-PA-1, System Biosciences) was transfected according to the protocol. Briefly, 2x10⁵ iPSC-MSCs or BM-MSCs were seeded one day before transfection. On the next day, lentiviral-mediated mitochondrial specific fragment fused with green fluorescence protein was added to 1 ml growth medium and incubated at 37 °C with a constant supply of 5% CO₂ for 16 hrs.

Flow cytometry analysis of mitochondrial transfer ratio

The mitochondrial transfer ratio from MSCs to NMCs was analyzed by fluorescence-activated cell sorting (FACS). Briefly, celltrace-labeled NMCs and mitotracker-labeled MSCs were co-cultured at a ratio of 1:1 in a 6-well plate with or without challenge of 1 μ M Dox and examined after 4, 12, 24 and 48 hrs. Data were acquired by FACS flow cytometry with a 488nm argon laser and a 405nm laser and

analyzed using CellQuest software. Moreover, the mitochondrial transfer ratio from MSCs to adult mice HL-1 cardiomyocytes or human AC16 cardiomyocytes was also examined after 24 hours co-culture. Unstained cells and labeled NMCs or MSCs alone were used for the set-up of FACScan.

Bioenergetic analysis of OCR

Bioenergetic Analysis of OCR of NMCs was measured by the Seahorse XF243 Extracellular Flux Analyzer (Seahorse Bioscience, North Billerica, MA) as described previously (Dier et al., 2014). NMCs were evenly seeded (8000 cells/well) onto the XF24 cell culture plate and allowed to attach for 24 hours. Cell culture media was replaced with XF media without sodium bicarbonate and FBS (Seahorse Bioscience). Prior to the start of the experiment, NMCs were placed in a non-CO₂ incubator for 1 hour. OCR was measured over a 3 minute period, followed by 3 mins mixing and re-oxygenation of the media.

Supplemental References

- Chan, Y.C., Tse, H.F., Siu, C.W., Wang, K., and Li, R.A. (2010). Automaticity and conduction properties of bio-artificial pacemakers assessed in an in vitro monolayer model of neonatal rat ventricular myocytes. *Europace* 12, 1178-1187.
- Cheng, K.K., Iglesias, M.A., Lam, K.S., Wang, Y., Sweeney, G., Zhu, W., Vanhoutte, P.M., Kraegen, E.W., and Xu, A. (2009). APPL1 potentiates insulin-mediated inhibition of hepatic glucose production and alleviates diabetes via Akt activation in mice. *Cell Metab.* 9, 417-427.
- Claycomb, W.C., Lanson, N.A., Stallworth, B.S., Egeland, D.B., Delcarpio, J.B., Bahinski, A., and Izzo, N.J. (1998). HL-1 cells: A cardiac muscle cell line that contracts and retains phenotypic characteristics of the adult cardiomyocyte. *Proc. Natl. Acad. Sci. USA* 95, 2979-2984.
- Davidson, M.M., Nesti, C., Palenzuela, L., Walker, W.F., Hernandez, E., Protas, L., Hirano, M., and Isaac, N.D. (2005). Novel cell lines derived from adult human ventricular cardiomyocytes. *J. Mol. Cell. Cardiol.* 39, 133-147.
- Dier, U., Shin, D.H., Hemachandra, L.P., Uusitalo, L.M., and Hempel, N. (2014). Bioenergetic analysis of ovarian cancer cell lines: profiling of histological subtypes and identification of a mitochondria-defective cell line. *PLoS One* 9, e98479.
- Liang, X., Ding, Y., Zhang, Y., Chai, Y.H., He, J., Chiu, S.M., Gao, F., Tse, H.F., and Lian, Q. (2015). Activation of NRG1-ERBB4 signaling potentiates mesenchymal stem cell-mediated myocardial repairs following myocardial infarction. *Cell Death Dis.* 6, e1765.